Global Journal of Environmental Science and Management
(GJESM)

Homepage: https://www.gjesm.net/

Podcasts

ORIGINAL RESEARCH ARTICLE

Satellite-based assessment of high Andean wetlands and carbon sequestration under the influence of climate change

Y. Mamani-Arpasi[1], J.A. Mamani Gomez[2,3], G. Huanca Chambi[1], M. Quispe Tisnado[1], C.E. Yupanqui Bendita[1], E. Calizaya Chura[1], E.G. Moreno Terrazas[4,*]

[1]*Universidad Nacional de Juliaca, San Román, 21101 Perú*

[2]*Institute for Research in Water Science and Technology, National University of Altiplano, Puno, 21001 Perú*

[3]*Faculty of Civil Engineering, Architecture and Urbanism, State University of Campinas, Campinas, 13083-970 Brazil*

[4]*Facultad de Ciencias Biológicas. Universidad Nacional del Altiplano, Puno, 21001 Perú*

ARTICLE INFO

Article History:
Received 12 May 2026
Revised 20 July 2026
Accepted 27 August 2026

Keywords:
Humidity
Rain
Temperature
Watershed
Wind

DOI:10. 22034.gjesm.2027.01.06

ABSTRACT

BACKGROUND AND OBJECTIVES: High-Andean wetlands play an important role in providing ecosystem services, particularly carbon sequestration. Yet, anthropogenic climate change threatens to restrict their spatial footprint and curtail their overall efficacy as atmospheric carbon sinks. Therefore, the study objectives were to estimate carbon uptake in High-Andean wetlands using satellite imagery and to evaluate its relationship with climatic variables in the Huancané Basin, Peru.

METHODS: Google Earth Engine and RStudio integrated development environment (v4.3.1) were used with JavaScript and R programming languages. Wetland extents were delineated across seasonal wet and dry phases via Linear Spectral Unmixing applied to Landsat 5–8 imagery. Subsequent to the conversion of digital numbers to surface reflectance, the wetland index was implemented to estimate carbon uptake using oderate resolution imaging spectroradiometer gross primary productivity and net primary productivity datasets. Climate data were obtained from the National Aeronautics and Space Administration power platform, and the relationships between wetland extent, carbon dioxide sequestration, and climatic variables were analyzed.

FINDINGS: Wetland coverage declined across both seasons over the study duration, experiencing contractions of 109.43 square kilometers during the wet season and 85.60 square kilometers during the dry season between 2010 and 2022. Carbon uptake also showed a decreasing trend during both seasons. Values ranged from 9.985 to 28.234 kilograms of carbon per square meter during the wet season and from 7.091 to 19.103 kilograms of carbon per square meter during the dry season. Significant relationships were found between wetland extent, carbon uptake, and climatic variables ($p<0.05$). Arid climatic trends, characterized by diminished precipitation, elevated temperature ranges, lower relative humidity, and increased wind speeds, corresponded closely with contractions in wetland extent and reduced carbon uptake.

CONCLUSION: The results indicate that recent climatic changes have contributed to the degradation of high-Andean wetlands and to a reduction in their carbon uptake capacity in the Huancané Basin. These results provide vital baselines for tracking wetland trajectories, informing climate change mitigation and conservation frameworks to guide future ecosystem management and sustainable planning in fragile mountain regions worldwide.

This is an open access article under the CC BY license (http://creativecommons.org/licenses/by/4.0/)

NUMBER OF REFERENCES	NUMBER OF FIGURES	NUMBER OF TABLES
46	7	4

*Corresponding Author:
Email: emoreno@unap.edu.pe
Phone: +51 951 677 041
ORCID: 0000-0001-6356-8806

Note: Discussion period for this manuscript open until March 01, 2027 on GJESM website at the “Show Article”.

INTRODUCTION

High-Andean wetlands play a key role in the provision of ecosystem services (Huaraca *et al.,* 2025), and are often regarded as oases because they sustain life in these arid environments (de la Fuente *et al.,* 2021). These ecosystems also contribute to the regional carbon balance, mainly through their capacity to accumulate organic matter (Malerba *et al.,* 2023; Ghosh *et al.,* 2025; Zhang *et al.,* 2025a), which is generally associated with plant communities dominated by cushion plants and grasses (Chimner, 2020). Within these systems, water availability and low thermal regimes sustain biological activity and carbon fixation across soils and vegetation, thereby modulating atmospheric carbon dioxide (CO_2) fluxes. (Suárez Duque *et al.,* 2016; Wicaksono *et al.,* 2016). Their functioning is therefore influenced by variations in water availability, temperature, and anthropogenic pressures such as grazing and fire (Garcia and Otto, 2015; Chimner, 2020; Huaraca *et al.,* 2025). Carbon storage and carbon dynamics in wetlands vary according to ecosystem type, vegetation cover and hydrological conditions (Cui *et al.,* 2021; Vorobyev *et al.,* 2024). This coupling has been extensively characterized across forest ecosystems (He *et al.,* 2022) as well as within marine-terrestrial transitional zones, with particular emphasis on blue carbon dynamics in coastal wetlands (Padhy *et al.,* 2020; Hamzeh and Azizi, 2023; Malerba *et al.,* 2023; Antony *et al.,* 2025; Chen *et al.,* 2025). In this context, carbon stock refers to the amount of carbon stored in a defined ecosystem pool, whereas carbon flux describes the transfer of carbon between the ecosystem and the atmosphere over time. Whereas Carbon sequestration denotes the net accumulation of carbon in an ecosystem, productivity signifies the rate of vegetation-mediated carbon; consequently, this study, centers on carbon uptake derived from MODIS productivity metrics, as opposed total ecosystem carbon stocks or net carbon sequestration. In addition, seasonal hydrological cycles influence carbon storage processes (Cui *et al.,* 2021). In floodplain environments, carbon emissions may exceed the amount of carbon stored (Das *et al.,* 2024; Vorobyev *et al.,* 2024), as previously accumulated carbon can be released through degradation processes (Senger *et al.,* 2021). These structural modifications complicate the derivation of reliable estimates regarding actual wetland carbon storage (Ghosh *et al.,* 2025). Therefore, this factor should be considered when assessing carbon storage in these ecosystems. Hitherto, research on carbon storage in High-Andean wetlands has relied primarily on vegetation biomass estimates and radiocarbon dating (Hribljan *et al.,* 2015; Llanos *et al.,* 2026). Although informative, these approaches have limitations, including high costs, restricted temporal coverage and complex procedures for long-term assessments. Consequently, there is a pressing need for accessible methodologies that enable scalable, large-scale monitoring. Remote sensing has become a widely used tool for evaluating changes in wetland extent, surface moisture and vegetation cover through the integration of optical and radar imagery, as well as for monitoring phenological dynamics using Landsat-Sentinel harmonisation and structural analyzes (He *et al.,* 2022; Malerba *et al.,* 2023; Fan *et al.,* 2023; Choi *et al.,* 2024; Ingalls *et al.,* 2024; Antony *et al.,* 2025; Shinkarenko and Bartalev, 2025). In this study, high-Andean wetlands are defined as water-saturated ecosystems characterized by hydrological regimes that drive vegetation dynamics and associated ecological processes. Furthermore, hotspot identification and CO_2 emission assessments have been conducted using UAV sensors, neural networks and spectral indices to estimate aboveground biomass and quantify the contribution of submerged vegetation (Belloli *et al.,* 2022; Liu *et al.,* 2023; Chen *et al.,* 2025; Li *et al.,* 2025;). Land-use change monitoring systems and greenhouse gas emission assessments also support regional inventories and climate targets

(Wannasiri and Chaksan, 2023; Zhang *et al.,* 2025a). Together, these methodologies provide efficient, scalable frameworks for assessing net carbon assimilation and functional dynamics of High-Andean wetlands, overcoming the principal constraints of conventional approaches. In this context, the High-Andean wetlands of the Huancané Basin represent strategic ecosystems because of their carbon storage capacity and marked seasonality. The novelty of this study lies in the integrated assessment of High-Andean wetland extent and carbon uptake across wet and dry seasons using multi-temporal Landsat and MODIS data, together with their associations with climatic variability in the Huancané Basin. This approach provides a basin-scale assessment of temporal variations in wetland extent and carbon uptake within a High-Andean ecosystem where such empirical data remains limited. The primary objectives of this study are to evaluate spatial variations in wetland extent, quantify net carbon assimilation by wetland vegetation, analyze the relationships among wetland coverage, net carbon uptake, climate-induced environmental variables. This study was carried out in the Huancané Basin, Peru, in 2010-2022.

MATERIALS AND METHODS

Study area

The Huancané watershed, located in the Puno Region, Peru, covers an area of 3,633.52 square kilometers (km²) and ranges in elevation from 3,806 meters above sea level (m a.s.l.) to 5,059 m a.s.l., at Surupana Hill. The geology is diverse and includes Cretaceous formations such as Huancané, Chupa, Muni and Moho, as well as the Cotacucho, Muñani and Vilquechico groups. Agricultural land occupies 414.04 km² with 11.40 percent (%) of the watershed in the lower areas and is characterised by low agricultural suitability, although it is used for grazing and permanent crops. The climate is cold and very humid, with annual precipitation ranging from 650 to 700 millimeters (mm) and mean temperatures between 4.5 and 5.2 degrees Celsius (°C). The dominant vegetation comprises High-Andean grasslands, whereas the hyperhumid subtropical subalpine páramo constitutes the primary ecological zone, covering more than half of the watershed. The region shows marked seasonality, with a wet season from November to March and a dry season from April to October (Fig. 1). The distribution of High-Andean wetlands is concentrated primarily within the upper sections of the Huancané Basin, restricted to localities exhibiting supportive hydrological conditions and seasonal water retention. Their spatial distribution is heterogeneous across the basin, reflecting differences in elevation, topography and local hydrological conditions.

Assessment of wetland extent

Wetland extent during the wet and dry seasons (2010–2022) was estimated using Landsat 5 Thematic Mapper (TM) and Landsat 8 Operational Land Imager (OLI) imagery with a spatial resolution of 30 meters (m). Landsat 5 TM and Landsat 8 OLI imagery were obtained from Google Earth Engine and converted from digital numbers to top-of-atmosphere (TOA) reflectance prior to spectral-index calculation. Mosaic and clip workflows were implemented within Google Earth Engine (GEE) to derive composite imagery covering the Huancané Basin. Only images with cloud cover below 10% were used. The corresponding Landsat sensor was used for each year of the study period. The geospatial tools, data sources, and analytical purposes used in the study are summarized in Table 1. Wetland extent was derived from Landsat-based spectral indices, whereas carbon uptake was estimated independently from MODIS productivity products, ensuring that wetland classification and area estimates were not employed as input variables for estimating carbon uptake calculations. The imagery was processed in RStudio integrated development environment (RStudio) using the normalized difference vegetation index (NDVI), normalized difference water index (NDWI) and NDII spectral indices to

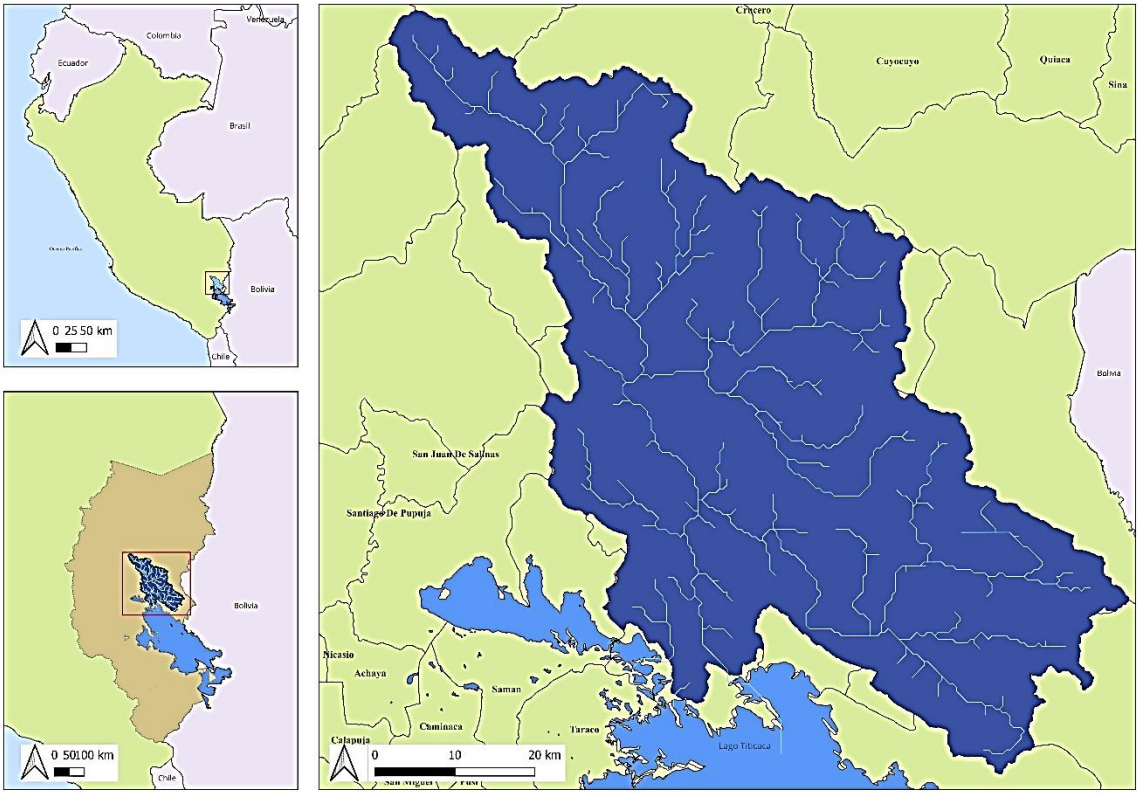

Fig. 1: Geographic location of the study area in the Huancané Basin, Puno Region in Peru

Table 1: Data sources and geospatial tools

Tool	Purpose	Data used
Google Earth Engine (JavaScript)	Satellite image processing, area calculation, GPP/NPP estimation	Landsat 5 and 8, MODIS (GPP, NPP)
RStudio v4.3.1	Spectral index calculation and statistical analysis (NDVI, NDWI, NDII, WI)	Satellite imagery and climatic time series
NASA power	Historical meteorological data	Temperature, precipitation, humidity and wind

characterize vegetation, vegetation water content and soil moisture, respectively (Table 2). The linear spectral unmixing (LSU) method was employed to generate the wetland index (WI) and classify wetland pixels, with the WI computed by integrating spectral data from the NDWI and NDII in accordance with the R-based analytical framework. The resulting WI was used to identify and delineate wetland areas during the wet and dry seasons. The resulting wetland extent was calculated for each year and season from the delineated wetland areas. The absence of independent quantitative accuracy evaluations and reference sample datasets precluded formal validation of the wetland classification across the study period. The uncertainty associated with the remote-sensing estimates was considered in relation to the characteristics of the datasets and processing steps used in the analysis. Potential errors in classifying wetlands could arise due to difficulties in spectrally resolving pixels alongside the spatial complexity found within the 30 m Landsat imagery. For carbon uptake, uncertainty is associated with the spatial and temporal characteristics of the MODIS productivity products and their conversion to carbon units.

Table 2: Spectral indices used for wetland assessment

Index	Application
$\text{NDVI} = \frac{\rho\text{NIR} - \rho\text{RED}}{\rho\text{NIR} + \rho\text{RED}}$	Vegetation
$\text{NDWI} = \frac{\rho\text{GREEN} - \rho\text{NIR}}{\rho\text{GREEN} + \rho\text{NIR}}$	Vegetation water content
$\text{NDII} = \frac{\rho\text{NIR} - \rho\text{SWIR}}{\rho\text{NIR} + \rho\text{SWIR}}$	Soil moisture

Furthermore, disparities in spatial resolution between Landsat and MODIS data may influence the alignment between wetland extent and carbon uptake estimates. These sources of uncertainty were considered when interpreting temporal patterns and relationships between wetland extent, carbon uptake and climatic variables. The wetland classification reflects aggregate spatial coverage and does not differentiate between distinct wetland typologies or internal ecological conditions within the mapped domain.

Estimation of Carbon Uptake

JavaScript was used within the GEE platform to evaluate the net primary productivity (NPP) of wetland vegetation as an indicator of carbon uptake. MODIS products from NASA's Earth Observing System (EOS) were used for this analysis. The MOD17A2HGF 8-Day Global 500 m product, which provides gross primary productivity (GPP), and the MOD17A3HGF Annual Global 500 m product, which provides annual NPP, were used. The Landsat-derived wetland polygons were imported into GEE and used as spatial masks to clip the MODIS productivity layers, restricting the carbon uptake estimates to the mapped wetland areas. Because of the difference in spatial resolution between Landsat (30 m) and MODIS (500 m), MODIS pixels along wetland boundaries may contain mixed land-cover information, which was considered as a methodological limitation. An algorithm workflow was implemented within GEE to approximate NPP at an 8-day temporal resolution by allocating annual NPP proportionally based on the relative contribution of each 8-day interval to total annual GPP using Eq. 1 (Ouattara *et al.*, 2025):

$$NPP_{8d} = \left(\frac{GPP_{8d}}{GPP_{anual}}\right) xNPP_{annual} \quad (1)$$

This technique operated on the assumption that the temporal progression of annual NPP followed the relative share contributed by each 8-day period to annual GPP. The resulting 8-day NPP estimates were then aggregated according to the corresponding wet and dry seasons. The resulting NPP values were quantified in kilograms of carbon per square meter (kg C/m²) and utilized to assess variations in carbon uptake between the wet and dry seasons. The spectral indices were calculated from the Landsat reflectance bands, and the Bofedal Index (BI) was subsequently derived from the combination of NDWI and NDII using the normalized-difference formulation. Specifically, NDWI was calculated from Landsat 5 bands 4 and 2, while NDII was calculated from bands 5 and 4. The derived indices were subsequently integrated to calculate the BI, which served to delineate wetland extents across both the wet and dry seasons. The complete methodological workflow, including Landsat processing, wetland delineation, MODIS productivity estimation, and seasonal carbon-uptake assessment, is presented in Fig. 2.

Analysis of environmental variables and climate change

Meteorological data were obtained from the NASA POWER database for the Huancané Basin. Climate data were extracted for a representative location within the basin (15.0743° S, 69.6493° W; 4,258 m a.s.l.), selected through remote sensing analysis in an open area free from topographic and structural obstructions. Monthly and annual records spanning 2010–2022 were compiled, including accumulated precipitation (mm), maximum and minimum temperature (°C), relative humidity (%), and wind speed (m/s) to assess climatic variability over the study period.

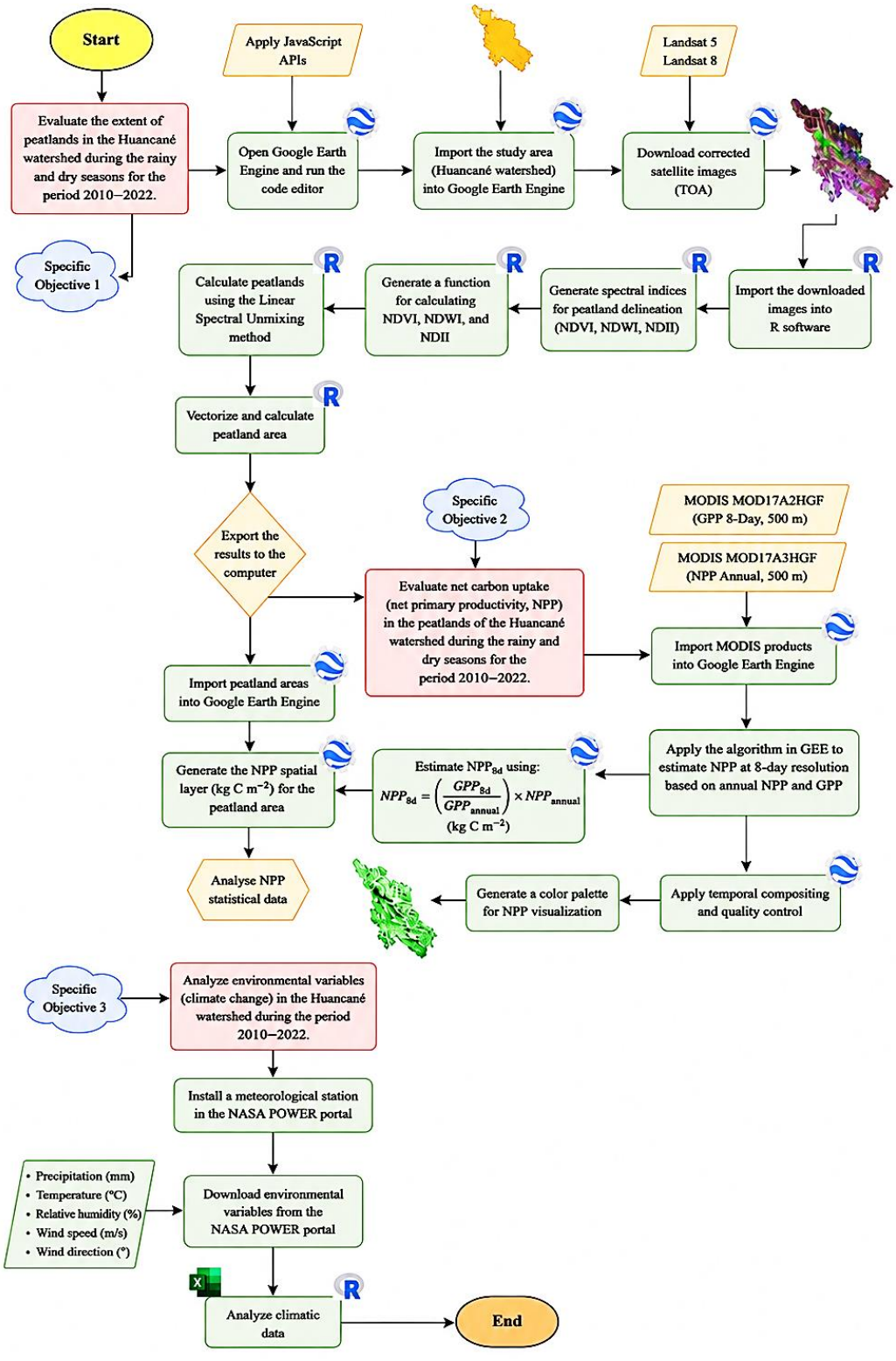

Fig. 2: Methodological workflow

Statistical analysis

Inferential statistics were used to evaluate the associations between Carbon uptake, wetland extent and climatic variables. Data normality was assessed using the Shapiro–Wilk test ($\alpha = 0.05$). Pearson correlation analysis was then applied to evaluate the linear associations between Carbon uptake, wetland extent and climatic variables. Owing to the limited number of temporal observations spanning 2010 to 2022, the magnitude of the correlation coefficients was evaluated with appropriate circumspection.

RESULTS AND DISCUSSION

Assessment of wetland area in the Huancané Basin during the wet and dry seasons

The analysis of wetland area in the Huancané Basin during the wet season between 2010 and 2022 showed a decreasing trend. The maximum wetland extents were documented at the commencement of the study period, whereas the minimum values were registered during the concluding years. Wetland area ranged from 28.63 km² to 181.72 km², with a mean value of 129.42 km², showing a progressive reduction in wetland cover under wet conditions (Fig. 3A). A similar decrease was observed during the dry season, with lower values towards the end of the study period (Fig. 3B). Wetland area ranged from 21.77 km² to 116.26 km², with a mean value of 85.35 km², reflecting a marked contraction under dry conditions. Although a comparable overall trajectory was observed across both seasons (Fig. 3C), the magnitude of the reduction was more pronounced during the wet season. Interannual fluctuations were observed, with increases in 2013, 2017 and 2020, which were subsequently succeeded by a sustained downward trajectory through the final years of the investigation, culminating in minimum values in 2022. The results show a marked decrease in wetland area between 2010 and 2022 during both seasons, with a greater reduction in the most recent years. This contraction aligns with findings from other regions indicating that High-Andean wetlands exhibit pronounced vulnerability to climatic variability and anthropogenic pressures (Fan *et al.,* 2023; Shinkarenko and Bartalev, 2025). The observed decline was associated with changes in precipitation and temperature (Cui *et al.,* 2021; Zhang *et al.*, 2025b). However, anthropogenic factors such as agricultural expansion and grazing may also influence wetland extent, although these factors were not quantitatively assessed in the present study. The evidence suggests that variations in climate across the 2010–2022 study timeframe corresponded with alterations in wetland expanse and carbon uptake dynamics in the Huancané Basin. In recent years, glaciers have decreased and, in some areas of the Peruvian Andes, have disappeared completely (Chimner, 2020). Glacier changes may influence water availability in Andean wetland systems, although their specific contribution to water availability in the Huancané Basin was not quantified in this study (Fan *et al.,* 2023). Climate change also influences precipitation and evaporation (Cui *et al.,* 2021). Because rising temperatures can significantly alter evapotranspiration rates, thermal parameters are routinely integrated into climate-change projections and future environmental scenarios (Cui *et al.,* 2021; Ngoc Tu *et al.,* 2025). The temporal fluctuations observed in 2013, 2017 and 2020 (Fig. 3C) suggest a gradual contraction pattern with periods of temporary stability, which is characteristic of High-Andean wetlands exposed to prolonged water stress (Ngoc Tu *et al.,* 2025). These fluctuations may also be related to glacier recharge and soil infiltration processes, which later supply water to wetlands (Chimner, 2020; Das *et al.,* 2024). As demonstrated by Fan *et al.* (2023) and Shinkarenko and Bartalev (2025), High-Andean wetlands can undergo episodic expansions in spatial extent, whereas persistent constraints on water availability ultimately dictate the overarching contraction trajectory and shape long-term ecosystem carbon dynamics.

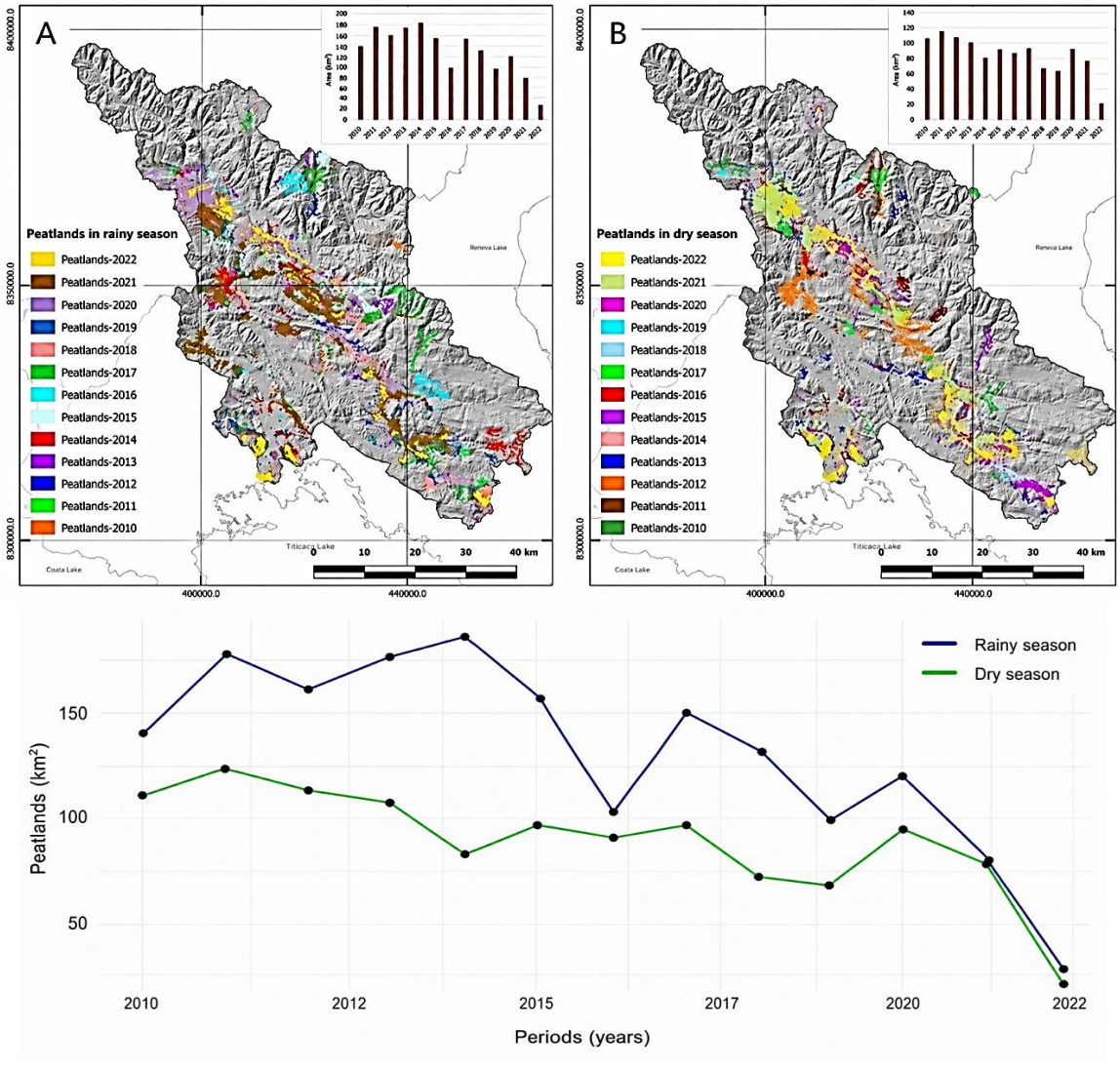

Fig. 3: Wetland area during the wet season (A) and dry season (B). Temporal variation in wetland area during the wet and dry seasons (C)

From an ecological perspective, the continued reduction in wetland area may affect aquatic vegetation, water retention, associated biogeochemical processes and biodiversity (Belloli *et al.,* 2022; Das *et al.,* 2024; Ghosh *et al.,* 2025). Fig. 4A shows the relationship between wetland area during the wet season and time. The linear regression equation shows a negative trend, with a coefficient of determination of R^2 = 0.615, indicating that 61.5% of the variation in wetland area is explained by time (Fig. 4A). Fig. 4B illustrates the relationship between dry-season wetland area and time, with the corresponding regression equation further confirming a negative trajectory. The coefficient of determination (R^2 = 0.624) indicates that 62.4% of the variation in wetland area is explained by time (Fig. 4B). These findings corroborate the aforementioned trends, wherein an inverse association was identified between precipitation and wetland extent. As water availability decreases, associated vegetation is reduced or lost, limiting the capacity of these ecosystems to sequester CO_2 and maintain long-term carbon storage.

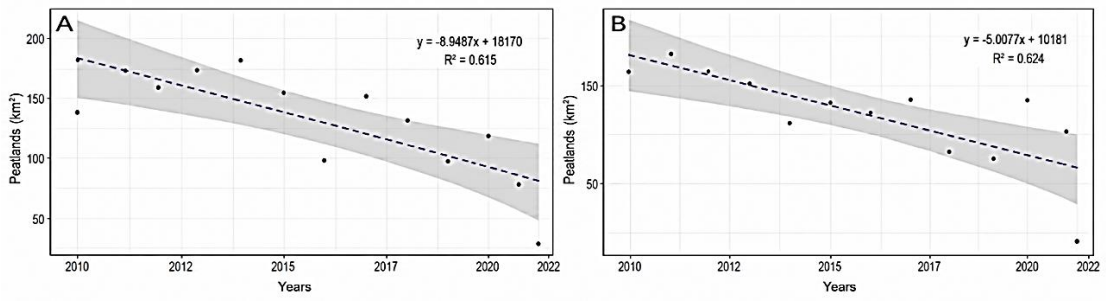

Fig. 4: Linear regression of wetland area during the wet season (A) and dry season (B) over time

Similar patterns have been reported in High-Andean wetlands of Ecuador and Peru, where reductions in water and vegetation cover are considered early indicators of ecosystem degradation (Chimner, 2020; Huaraca *et al.,* 2025). The negative trajectories documented across both seasons signify a broader reduction in wetland extent throughout the study period, notwithstanding interannual variability, with analogous spatial and temporal dynamics documented elsewhere in the Andes. For example, studies in wetlands of northern Chile based on long-term Landsat image series have shown that wetland area fluctuations are strongly influenced by interannual climatic variability associated with events such as the El Niño-Southern Oscillation (ENSO), as well as by the balance between groundwater recharge and potential evaporation. These processes drive decades-long cycles of wetland expansion and contraction over several decades (de la Fuente *et al.,* 2021), implying that the reductions documented in this study align with broader transformation patterns observed in High-Andean wetlands under varying climatic and hydrological conditions (Withaningsih *et al.*, 2026).

Assessment of net carbon uptake in the wetlands of the Huancané Basin

The results show that net carbon uptake fluctuated between 2010 and 2022, with an overall decreasing trend. The highest values were recorded at the beginning of the wet period and the lowest values towards the end of the study period, ranging from 9.985 to 28.234 kg C/m², with a mean value of 20.22 kg C/m², indicating high spatial and temporal variability (Fig. 5A). During the dry season, values ranged from 7.091 to 19.103 kg C/m² (mean = 13.658 kg C/m²; standard deviation = 3.300), showing moderate variability and an approximately normal distribution (Fig. 5B). The reduction in net carbon uptake was evident during both seasons and was more pronounced during the dry season (Fig. 5C). Carbon uptake in wetlands ranged from 7.091 to 28.234 kg C/m², showing high spatial and temporal variability. This heterogeneity reflects the contrasting structure and functioning of mountain wetlands. Previous remote-sensing studies have shown that similar environmental gradients generate distinct spatial patterns of carbon uptake (Junttila *et al.,* 2021; Belloli *et al.,* 2022). The combination of optical and radar sensors reinforces the inference that the detected variability stems from underlying ecological processes rather than methodological artefacts (Fan *et al.,* 2023; Shinkarenko and Bartalev, 2025). During periods of water deficit, photosynthesis capacity becomes constrained as plants close their stomata to minimize transpirational loss. Consequently, carbon assimilation decreases due to diminished photosynthetic rates (Llanos *et al.,* 2026), a pattern that aligns with wetland observations where climatic seasonality dictates interannual fluctuations in net CO_2 fluxes (Wang *et al.,* 2024; Zhang *et al.,* 2025b). Studies covering longer time periods have also reported significant changes in wetland extent, biomass and carbon

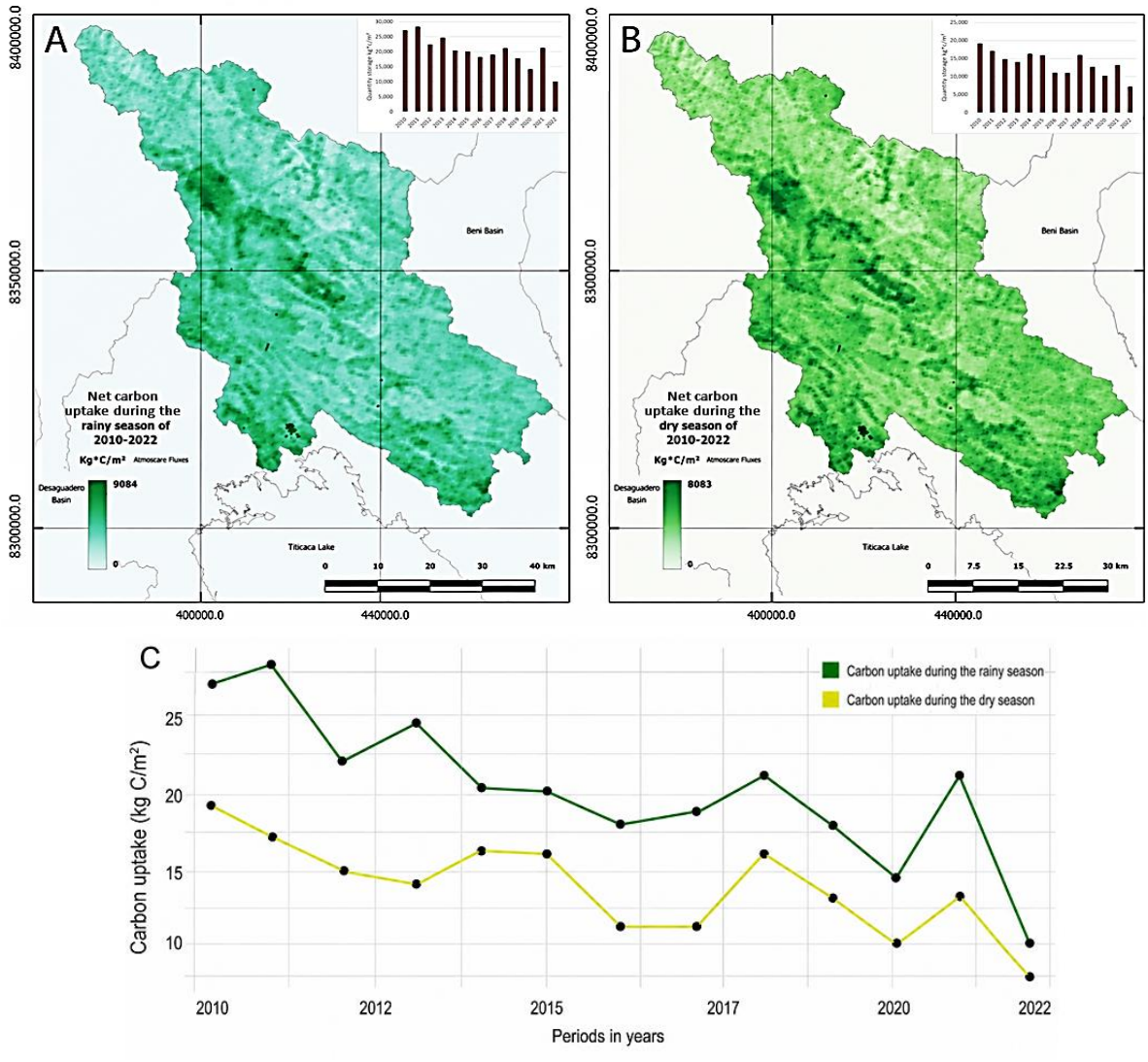

Fig. 5: Carbon uptake in wetlands during the wet season (A) and dry season (B) between 2010 and 2022, Temporal variation in net carbon uptake during the wet and dry seasons (C)

accumulation associated with hydroclimatic variability (de la Fuente *et al.,* 2021). These findings suggest that the decline in Carbon uptake observed in the Huancané Basin is consistent with responses reported for wetlands under changing environmental conditions and that these ecosystems do not respond linearly to changing climatic conditions. Methodologically, remote sensing provides a robust framework for connecting spectral indices and biomass metrics to ecosystem carbon dynamics (Senger *et al.,* 2021; Malerba *et al.,* 2023; Ngoc Tu *et al.,* 2025). This interpretation aligns with prior studies demonstrating that wetlands exhibit extreme vulnerability to hydrological disruptions, wherein minor fluctuations in water availability can induce substantial shifts in carbon storage (Christiani *et al.,* 2024). Studies from other regions have reported carbon values that provide a broader context for the estimates obtained in this study (7.091–28.234 kg C/m²), although differences in ecosystem type and carbon pools should be

considered. In Colombia, values between 0.7 and 1.5 kg C/m² were reported (Peña *et al.,* 2009). In Huascarán National Park, average values of 3 kg C/m² were reported for wet meadows and 109.2 kg C/m² for peatlands (Chimner *et al.,* 2023). In Bolivia, values of 104 kg C/m² in Manasaya and 57.2 kg C/m² in other wetland areas were reported (Hribljan *et al.,* 2015). In Ecuador, values of 136.2 kg C/m² in Antisana and 164.7 kg C/m² in Cajas were reported (Suárez Duque *et al.,* 2016). The discrepancies noted among values reported for the Huascarán, Bolivian, and Ecuadorian peatlands are largely attributable to the accounting of subsurface peat deposits alongside aboveground vegetation. Conversely, studies conducted in Colombia concentrated on biomass and necromass rather than aggregate wetland carbon storage. These comparative insights underscore the critical role of biomass, necromass and peat deposits as primary carbon reservoirs in wetland ecosystems. The regression analysis showed a significant inverse relationship between time and Carbon uptake (kg C/m²). Detailed regression statistics are provided in Table 3. During the wet season, temporal progression accounted for 68.4% of the total variance ($R^2 = 0.684$), denoting a persistent reduction in wetland carbon sequestration efficiency (Fig. 6A). A similar negative trend was observed during the dry season (Fig. 6B), where the model explained 60.3% of the variation in carbon uptake ($R^2 = 0.603$). Additionally, a direct correlation analysis showed a positive association between wetland extent and carbon uptake during both the wet season ($r = 0.699$, $p = 0.0079$) and dry season ($r = 0.621$, $p = 0.0236$ (Table 4). This association indicates that years with greater wetland extent tended to coincide with higher carbon uptake. These correlations, however, do not infer causation, given that carbon uptake can be confounded or mediated by local vegetation attributes, soil properties and hydrological conditions. The negative relationship between time and carbon uptake suggests a progressive decline in the ecological functioning of the wetlands. Constrained water availability can suppress plant productivity and photosynthetic carbon fixation, ultimately reducing carbon sequestration over time. Comparable trends have been documented in High-Andean wetlands, where hydrological shifts govern vegetation cover, biomass accumulation, and overall carbon cycling (Wicaksono *et al.,* 2016; Hoyt *et al.,* 2020; Malerba *et al.,* 2023). The decline observed in the Huancané Basin is therefore likely to be associated with a gradual reduction in water availability, which may be affecting both vegetation productivity and the capacity of wetlands to carbon uptake. Although the regression analysis demonstrates a linear trend, the underlying mechanisms governing carbon uptake are inherently more complex, likely driven by multifaceted interactions among climatic factors, vegetation dynamics, and soil properties (Zhang, *et al.,* 2025b). Given the relatively short time series, linear regression was used to characterise the overall temporal trend rather than imply a strictly linear ecological response. This interpretation is consistent with previous studies showing that wetland responses can vary among periods and locations. For example, a multitemporal study of wetlands in the upper Santa River Basin demonstrated that observed ecological shifts were significantly associated with fluctuations in soil moisture and vegetation cover. Their results showed that wetland responses may differ among periods and sectors, even when the overall trend remains unchanged, reflecting the influence of spatial heterogeneity and temporal environmental variability on wetland ecological dynamics.Similarly, palaeoecological records from Andean peatlands revealed marked changes in carbon accumulation rates during particular decades (Garcia and Otto, 2015) suggesting that these ecosystems do not respond uniformly over time. Consequently, the linear trend observed in this study may represent the general behaviour of the system, while smaller-scale variations remain undetected by the model due to temporal resolution and inherent environmental variability.

Table 3: Temporal linear regression statistics for wetland extent and carbon uptake during 2010–2022

Response variable	Season	n	Slope	SE	95% CI for slope	R^2	p-value
Wetland extent (km²)	Wet	13	−8.949	2.135	−13.647 to −4.251	0.615	0.0015
Wetland extent (km²)	Dry	13	−5.008	1.172	−7.587 to −2.428	0.624	0.0013
Carbon uptake (kg C/m²)	Wet	13	−1.046	0.214	−1.518 to −0.575	0.684	0.0005
Carbon uptake (kg C/m²)	Dry	13	−0.658	0.161	−1.013 to −0.304	0.603	0.0018

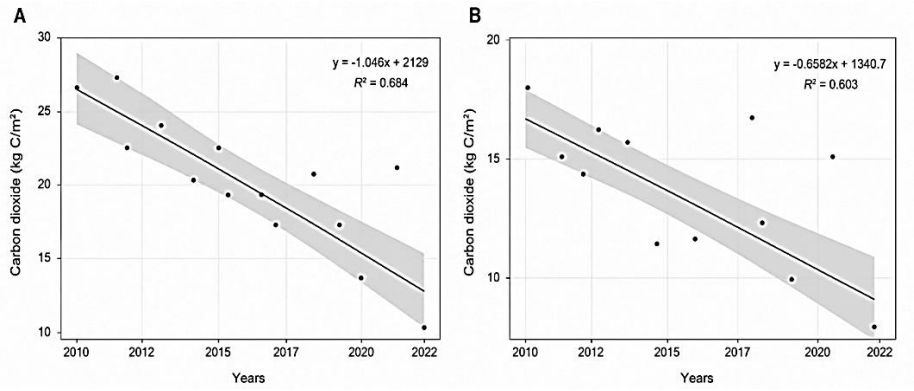

Fig. 6: 1 Linear regression of carbon uptake against time during the wet season (A) and dry season (B)

Table 4: Statistical analyzes of wetland extent, carbon uptake and environmental variables during 2010–2022

Variable / relationship	Season	n	Pearson's *r*	95% CI	p-value
Cumulative precipitation (mm)	Wet	13	0.91	0.72–0.97	2×10^{-5}
Cumulative precipitation (mm)	Dry	13	0.89	0.67–0.97	5.4×10^{-5}
Maximum temperature (°C)	Wet	13	−0.79	−0.93–−0.42	0.0009
Maximum temperature (°C)	Dry	13	−0.78	−0.93–−0.40	0.0016
Relative humidity (%)	Wet	13	0.80	0.45–0.94	0.0011
Relative humidity (%)	Dry	13	0.75	0.34–0.92	0.003
Wind speed (m/s)	Wet	13	−0.78	−0.93–−0.40	0.0015
Wind direction (°)	Dry	13	−0.86	−0.96–−0.59	4×10^{-5}
Wetland extent (km²)	Wet	13	0.699	0.240–0.902	0.0079
Wetland extent (km²)	Dry	13	0.621	0.106–0.873	0.0236

The seasonal analysis suggests that carbon dynamics extend beyond cyclical intra-annual variations to encompass broader interannual trends. Supported by correlation metrics showing positive associations between precipitation and carbon uptake in both wet (r = 0.91) and dry season (r = 0.88) season, these results indicate that increased moisture availability acts as a primary catalyst for elevated carbon sequestration (Figs. 7A and B). This pattern is consistent with observations from mountain wetlands, where the dry season acts as a critical period that amplifies cumulative respiratory losses (de la Fuente *et al.,* 2021). From an ecological perspective, the carbon balance becomes particularly vulnerable during dry conditions. From a methodological perspective, remote-sensing-based regression assumes a stable relationship between spectral response, biomass and carbon storage. Previous studies indicate that this relationship is suitable for detecting interannual trends, although uncertainty remains because of spatial heterogeneity and phenological variability (Shinkarenko and Bartalev, 2025). Therefore, the R^2 values primarily indicate temporal consistency of the observed pattern rather than absolute ecological precision under field conditions, where spatial heterogeneity, measurement uncertainty, and seasonal variability may influence relationships and interpretations.

Environmental variable analysis of climate change in the Huancané Basin

During the study period, annual precipitation decreased from 1289.8 mm in 2012 to 626.5 mm in 2022, with a mean value of 989.31 ± 180.98 mm, indicating a sustained reduction in water inputs and moderate interannual variability. Temperature showed a progressive increase, rising from 7.89 °C in 2011 to 14.89 °C in 2022. Mean maximum temperature was 11.42 ± 2.03 °C, whereas mean minimum temperature was −0.01 ± 0.57 °C. Relative humidity decreased from 83.98% in 2011 to 72.78% in 2022, with a mean value of 78.63 ± 3.24%, reflecting a shift towards drier conditions. Wind speed remained relatively stable (2.07 ± 0.05 m/s) (Fig. 7). Correlation analysis revealed robust positive associations between carbon uptake and annual precipitation during both the wet (r = 0.91) and dry (r = 0.89) seasons. Similarly, relative humidity exhibited positive correlations with carbon uptake during the wet (r = 0.80) and dry (r = 0.75) season. Conversely, temperature demonstrated a strong negative correlation with carbon uptake during in both seasons (r = −0.83), indicating that elevated temperatures constrain carbon assimilation (Table 4). Relative humidity and precipitation emerge as critical environmental determinants controlling vegetation development and, consequently, carbon fixation pathways. Studies in wetlands of northern Chile have shown that prolonged dry periods are associated with higher carbon losses, suggesting that reduced precipitation may increase CO_2 release through respiration and organic matter decomposition under less anoxic conditions (de la Fuente *et al.,* 2021; Syamdidi *et al.,* 2026). Alterations in precipitation regimes can additionally modulate the decomposition rates (Llanos *et al.,* 2026). In Huascarán National Park, wetland types with greater water saturation, such as peatlands, were found to store substantially larger amounts of carbon than less saturated wet meadows (Chimner *et al.,* 2023). Similarly, studies of Andean peatlands have shown that deep carbon deposits develop under long-term saturated conditions (Hribljan *et al.,* 2015; Benavides *et al.,* 2023). Together, these findings highlight the importance of hydrological regimes in modulating carbon storage dynamics across High-Andean wetlands. Temperature and wind speed showed negative associations with carbon uptake during the study period. For instance, a prior study reported a decline in carbon accumulation over a 65-year period preceding 1980, driven by regional warming that accelerated organic matter degradation in response to broader climatic shifts and glacier retreat. These processes altered the hydrological flows required for wetlands to maintain their function as carbon sinks (Llanos *et al.,* 2026). Elevated temperatures can accelerate organic matter decomposition rates and ecosystem respiration, thereby enhancing carbon release to the atmosphere (Junttila *et al.,* 2021; Masocha and Mhangara, 2025). These results support the importance of temperature and precipitation as key variables in studies of carbon storage and carbon uptake in wetland ecosystems (Chen *et al.,* 2025; Ngoc Tu *et al.,* 2025), consistent with evidence that land-use changes can alter ecosystem carbon stocks (Ketaren *et al.,* 2026).

Hydrological trends and implications

From a climatic perspective, regional evidence supports the pattern identified in this study. Studies of hydroclimatic fluctuations within the tropical Andes indicate a projected rise in both the occurrence and magnitude of droughts in southern Peru (Vuille *et al.,* 2018; IPCC, 2021). At a global scale, Johnson *et al.* (1999) reported that wetlands associated with the Herbert River in Australia declined by 70% between 1943 and 1996. Additionally, assessments by the IPCC underscore the pronounced susceptibility of diverse wetland ecosystems to climate change driven by their strict dependence on sustained water availability and hydrological equilibrium (Garcia and Otto, 2015). Reduced water availability restricts vegetation productivity and limits carbon assimilation, while structural

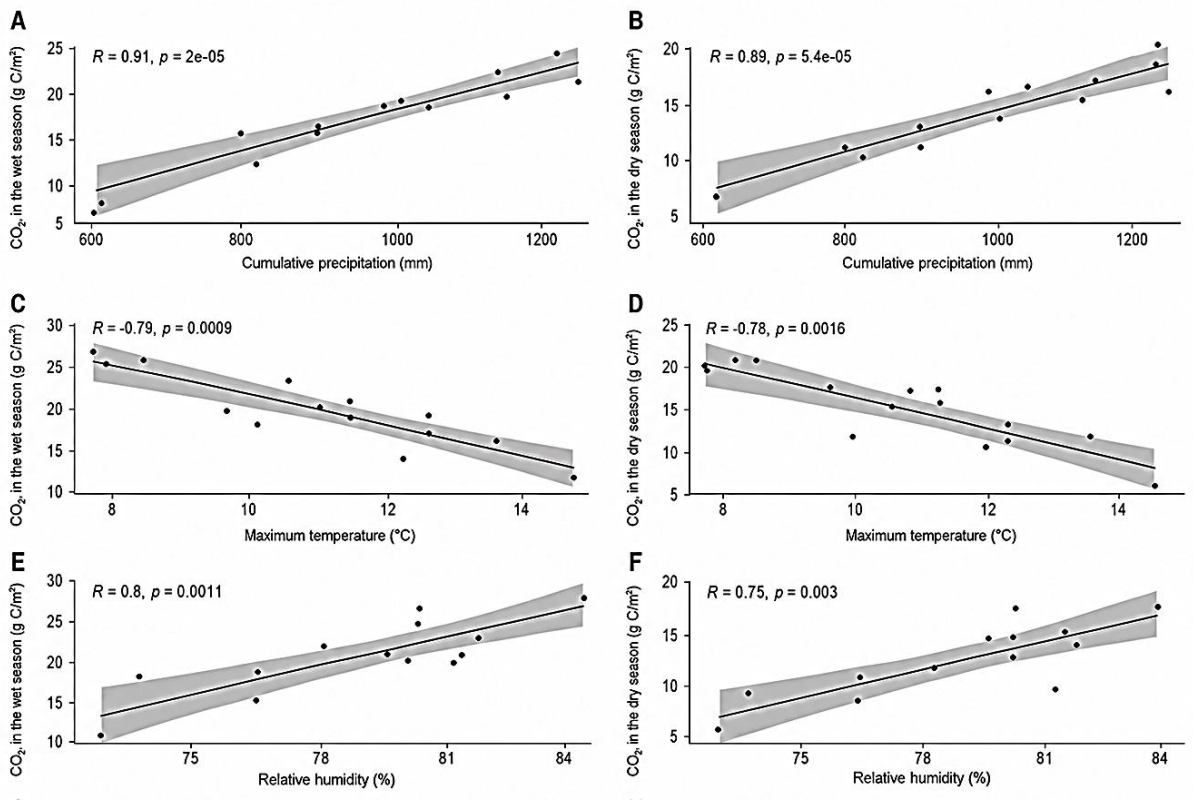

Fig. 7: Correlation between carbon uptake and environmental variables during the wet season (left column) and dry season (right column). Precipitation (A, B), temperature (C, D), relative humidity (E, F)

changes in plant communities further modify ecosystem carbon storage. Such trends align with impairment stimulates the oxidation of organic matter, driving the release of CO_2 and auxiliary greenhouse gases (Hribljan *et al.,* 2015). When wetlands experience prolonged loss of saturation, their capacity to function as carbon sinks may decline, increasing net carbon emissions. These changes have important implications for climate-change mitigation. Overall, scientific evidence indicates that wetlands are highly vulnerable to climate change because of their dependence on hydrological balance and sensitivity to drought and warming (López-Moreno *et al.,* 2017).

CONCLUSION

Wetland extent decreased in the Huancané Basin between 2010 and 2022 in both seasons. The decrease was 109.43 km² in the wet season and 85.60 km² in the dry season. Carbon uptake also showed a decreasing trend during this period. Values ranged from 9.985 to 28.234 kg C/m² in the wet season and from 7.091 to 19.103 kg C/m² in the dry season. The temporal regression modeling demonstrated that variations in time explained 68.4% of carbon uptake dynamics within the wet season and 60.3% during the dry season. Accordingly, parallel reductions in wetland extent and carbon uptake were recorded throughout the study duration. The substantial decrease in wetland extent during the wet season demonstrates that hydrological contractions were not confined to the dry period, manifesting instead across the full seasonal cycle. Wetland extent was positively correlated with carbon uptake in both seasons. The correlation was r = 0.699 in the wet season and r = 0.621 in the dry season. Interannual comparisons indicate that years featuring more extensive wetland coverage generally demonstrated enhanced carbon

sequestration capacity. However, this relationship does not indicate that reduced wetland area directly caused decreased carbon uptake. Carbon uptake is also influenced by vegetation characteristics, soil properties, and hydrological conditions; therefore, changes in wetland extent should be evaluated alongside these factors. During the study period, precipitation and relative humidity decreased, while temperature increased. Carbon uptake was positively correlated with precipitation and relative humidity and negatively correlated with temperature in both seasons, indicating that water availability and temperature were associated with temporal variation in carbon uptake in these High-Andean wetlands. The persistence of these inter-seasonal relationships suggests a consistent climatic influence on carbon assimilation across the annual cycle. However, as the study relied on observational satellite and climatic data, these relationships should be interpreted as associations rather than causal effects. The relative contributions of climate variability, natural variability, and anthropogenic pressures cannot be separated under the current study design. The use of Landsat imagery, MODIS productivity products, Google Earth Engine and NASA POWER data allowed changes in wetland extent and carbon uptake to be evaluated over the 2010–2022 period. The combination of these datasets was useful for examining wetland dynamics together with climatic conditions across the Huancané Basin. Landsat provided the spatial information required to evaluate changes in wetland extent, while MODIS productivity products allowed carbon uptake to be examined over the same period. However, the difference in spatial resolution between Landsat and MODIS and the lack of independent field validation should be considered when interpreting the estimates. Such constraints assume particular relevance when correlating wetland extent with carbon uptake, given that the respective datasets resolve the ecosystem across differing spatial scales. The decrease in wetland extent and carbon uptake observed in the Huancané Basin shows the need to keep monitoring these ecosystems. In particular, changes in precipitation, temperature and water availability should be followed over time. Furthermore, ground-truth data on vegetation biomass, soil moisture, and edaphic carbon stocks would strengthen cross-validation of satellite estimates and improve understanding of ecosystem carbon uptake. Additional information on elevation, land use, and human activities could further explain basin-scale differences. Extending the time series would help determine whether the observed 2010–2022 decline is continuing. Future monitoring combining ground-based observations with satellite telemetry could provide higher-resolution assessments of wetland dynamics and carbon sequestration and clarify whether the Huancané Basin trends reflect ongoing change or longer-term variability in High-Andean wetland ecosystems.

AUTHOR CONTRIBUTIONS

Y.M. Mamani-Arpasi conceived the study, developed the methodology, conducted the investigation, curated the data, performed the formal analysis, prepared the visualizations, and prepared the original manuscript draft and revised the manuscript. J.A. Mamani Gomez contributed to the methodology, performed validation, and reviewed and edited the manuscript. G. Huanca Chambi performed validation, provided resources, and reviewed and edited the manuscript. M. Quispe Tisnado curated the data, performed validation, and reviewed and edited the manuscript. C.E. Yupanqui Bendita provided resources, performed validation, and reviewed and edited the manuscript. E. Calizaya Chura performed validation and reviewed and edited the manuscript. E.G. Moreno Terrazas supervised the study, contributed to the methodology, performed validation, administered the project, and reviewed and edited the manuscript.

ACKNOWLEDGEMENT

Authors would like to thank the Universidad Nacional de Juliaca, San Román as well as Institute for Research in Water Science and Technology,

National University of Altiplano, Perú. This study received no external funding.

CONFLICT OF INTEREST

The authors declare that there is no conflict of interest regarding the publication of this manuscript. In addition, ethical issues, including plagiarism, informed consent, misconduct, data fabrication and/or falsification, double publication and/or submission, and redundancy, were observed by the authors.

OPEN ACCESS

©2027 The author(s). This article is licensed under a Creative Commons Attribution 4.0 International License, which permits use, sharing, adaptation, distribution and reproduction in any medium or format, as long as you give appropriate credit to the original author(s) and the source, provide a link to the Creative Commons license, and indicate if changes were made. The images or other third-party material in this article are included in the article's Creative Commons license, unless indicated otherwise in a credit line to the material. If material is not included in the article's Creative Commons license and your intended use is not permitted by statutory regulation or exceeds the permitted use, you will need to obtain permission directly from the copyright holder. To view a copy of this license, visit: http://creativecommons.org/licenses/by/4.0/

PUBLISHER'S NOTE

GJESM Publisher remains neutral with regard to jurisdictional claims in published maps and institutional affiliations.

NEGATIVE AI STATEMENT

The authors declared that no AI tools or services were used or not highly applied during the preparation of this work.

ABBREVIATIONS

%	Percent
°C	Degrees Celsius
CO_2	Carbon dioxide
ENSO	El Niño–Southern Oscillation
EOS	Earth observing system
GEE	Google Earth Engine
GPP	Gross primary productivity
IPCC	Intergovernmental Panel on Climate Change
kg	Kilogram
kg C/m²	Kilograms of carbon per square meter
km	Kilometer
km²	Square kilometer
LSU	Linear spectral unmixing
m	Meter
m a. s. l.	Meter above sea level
M/s	Meters per second
mm	Millimeter
MODIS	Moderate resolution imaging spectroradiometer
NASA	National Aeronautics and Space Administration
NDII	Normalized difference infrared index
NDVI	Normalized difference vegetation index
NDWI	Normalized difference water index
NPP	Net primary productivity
OLI	Operational land imager
POWER	Prediction of Worldwide Energy Resources
R^2	Coefficient of determination
RStudio	RStudio integrated development environment
%	Percent
TM	Thematic mapper
TOA	Top of atmosphere
WI	Wetland index

REFERENCES

Antony, S.; Perumal, K.; Devi, S.S.; Shajahan, S.; Kumar, A.B., (2025). Exploring blue carbon research in India: current landscape and future avenues. Mar. Pollut. Bull., 219: 118269 **(18 pages).**

Belloli, T.F.; Guasselli, L.A.; Kuplich, T.M.; Ruiz, L.F.C.; Arruda, D.C.; Etchelar, C.B.; Simioni, J.D., (2022). Estimation of aboveground biomass and carbon in palustrine wetland using bands and multispectral indices derived from optical satellite imageries PlanetScope and Sentinel-2A. J. Appl. Remote Sens., 16(3): 034516 **(21 pages).**

Benavides, J.C.; Vitt, D.H.; Cooper, D.J., (2023). The High-Elevation Peatlands of the Northern Andes, Colombia. Plants. 12(4): 955 **(17 pages).**

Chen, J.; Lu, Y.; Liu, F.; Gao, G.; Xie, M., (2025). Remote sensing evidence of blue carbon stock increase and attribution of its drivers in coastal China. Remote Sens., 17(15): 2559 **(22 pages).**

Chimner, R., (2020). Andes, bofedales, and the communities of Huascarán National Park, Peru. Wetl. Sci. Pract., 37(4): 246-254 **(9 pages).**

Chimner, R.A.; Resh, S.C.; Hribljan, J.A.; Battaglia, M.; Bourgeau-Chavez, L.; Bowser, G.; Lilleskov, E.A., (2023). Mountain wetland soil carbon stocks of Huascarán National Park, Peru. Front. Plant Sci., 14: 1-8 **(8 pages).**

Choi, I.H.; Lee, E.R.; Jung, H.S., (2024). Performance comparison of water body detection from Sentinel-1 SAR and Sentinel-2 optical imagery using Attention U-Net model. Korean J. Remote Sens., 40(5): 507-523 **(17 pages)**.

Christiani, P.; Rana, P.; Räsänen, A.; Pitkänen, T.P.; Tolvanen, A., (2024). Detecting spatial patterns of peatland greenhouse gas sinks and sources with geospatial environmental and remote sensing data. Environ. Manage., 74(3): 461-478 **(18 pages)**.

Cui, Q.; Ammar, M.E.; Iravani, M.; Kariyeva, J.; Faramarzi, M., (2021). Regional wetland water storage changes: The influence of future climate on geographically isolated wetlands. Ecol. Indic., 120: 106941 **(17 pages)**.

Das, T.; Pal, S.; Debanshi, S., (2024). Effect of water presence consistency on balance between CH4 emission and CO2 sequestration in floodplain wetland. Acta Geophys., 73(2): 1847-1864 **(18 pages)**.

de la Fuente, A.; Meruane, C.; Suárez, F., (2021). Long-term spatiotemporal variability in high Andean wetlands in northern Chile. Sci. Total Environ. 756, 143830 **(13 pages)**.

Fan, C.; Yang, J.; Zhao, G.; Dai, J.; Zhu, M.; Dong, J.; Liu, R.; Zhang, G., (2023). Mapping phenology of complicated wetland landscapes through harmonizing Landsat and Sentinel-2 imagery. Remote Sens., 15(9): 2413 **(19 pages)**.

Garcia, E.; Otto, M., (2015). Ecohydrological characterization of High-Andean wetlands based on multi-temporal remote sensing images in the case of Upper Santa River, Ancash, Peru. Ecol. Apl., 14(1-2): 115 **(11 pages).**

Ghosh, R.; Haldar, M.; Debanshi, S.; Pal, S., (2025). Role of ox-bow lakes towards carbon sink and resilience of warming effect. Spat. Inf. Res., 33(4): 6369-6392 **(13 pages).**

Hamzeh, M.A.; Azizi, N., (2023). Estimating blue carbon storage in the mangrove forest of Gaz-Harra wetland, Strait of Hormoz. Reg. Stud. Mar. Sci., 66: 103142 **(09 pages).**

He, L.; Byrne, B.; Yin, Y.; Liu, J.; Frankenberg, C., (2022). Remote-sensing derived trends in gross primary production explain increases in the CO2 seasonal cycle amplitude. Glob. Biogeochem. Cycles, 36(9) **(16 pages).**

Hoyt, A.M.; Chaussard, E.; Seppalainen, S.S.; Harvey, C.F., (2020). Widespread subsidence and carbon emissions across Southeast Asian peatlands. Nat. Geosci., 13(6): 435-440 **(06 pages).**

Hribljan, J.A.; Cooper, D.J.; Sueltenfuss, J.; Wolf, E.C.; Heckman, K.A.; Lilleskov, E.A.; Chimner, R.A., (2015). Carbon storage and long-term rate of accumulation in high-altitude Andean peatlands of Bolivia. Mires Peat, 15: 1-14 **(14 pages).**

Huaraca, L.; Bourrel, L.; Zapata-Ríos, X.; Páez-Bimos, S.; Lahuatte, B.; Galeas, R.; Fuentes, P.; Frappart, F., (2025). Multitemporal monitoring of Ecuadorian Andean high wetlands using radar and multispectral remote sensing. Water, 17(11): 1637 **(30 pages).**

Ingalls, T.C.; Li, J.; Sawall, Y.; Martin, R.E.; Thompson, D.R.; Asner, G.P., (2024). Imaging spectroscopy investigations in wet carbon ecosystems: A review of the literature from 1995 to 2022 and future directions. Remote Sens. Environ., 305: 114051 **(23 pages).**

IPCC, (2021). Ecosystems and conservation: Wetlands. Intergovernmental Panel on Climate Change.

Johnson, A.K.L.; Ebert, S.P.; Murray, A.E., (1999). Distribution of coastal freshwater wetlands and riparian forests in the Herbert River catchment and implications for management of catchments adjacent the Great Barrier Reef Marine Park. Environ. Conserv., 26(3): 229-235 **(07 pages).**

Junttila, S.; Kelly, J.; Kljun, N.; Aurela, M.; Klemedtsson, L.; Lohila, A.; Nilsson, M.B.; Rinne, J.; Tuittila, E.S.; Vestin, P.; Weslien, P.; Eklundh, L., (2021). Upscaling northern peatland CO2 fluxes using satellite remote sensing data. Remote Sens., 13(4): 1-23 **(23 pages).**

Ketaren, D.G.K.; Radjawane, I.M.; Latief, H.; Sidik, F.; Trenggono, S.W.; Diantara, S.D.; Setyawidati, N.A.R.; Akbar, M.I.; Raja, J.A.L.; Farkhan, M.A.; Kasim, K.; Maharani, S. (2026). Impacts of mangrove land-use change on carbon stocks in coastal ecosystems. Global J. Environ. Sci. Manage., 12(3): 1041-1060 **(20 pages).**

Li, Y.; Henrion, M.; Moore, A.; Lambot, S.; Opfergelt, S.; Vanacker, V.; Jonard, F.; Van Oost, K., (2025). Hot spots, hot moments, and spatiotemporal drivers of soil CO2 flux in temperate peatlands using UAV remote sensing. Biogeosciences, 22(21): 6369-6392 **(24 pages).**

Liu, B.; Sevick, T.; Jung, H.; Kiskaddon, E.; Carruthers, T., (2023). Quantifying the potential contribution of submerged aquatic vegetation to coastal carbon capture in a delta system from field and Landsat 8/9 Operational Land Imager (OLI) data with deep convolutional neural network. Remote Sens., 15(15): 3765 **(24 pages).**

Llanos, R.; Moreira-Turcq, P.; Turcq, B.; Cordeiro, R.; Espinoza-Villar, R.; Huaman-Navarro, Y.; Condom, T.; Willems, B., (2026). Drastic change in Andean peatland carbon accumulation in the 1980s. Glob. Earth Surf. Process. Change, 5: 100014 **(11 pages).**

López-Moreno, J.I.; Valero-Garcés, B.; Mark, B.; Condom, T.; Revuelto, J.; Azorín-Molina, C.; Bazo, J.; Frugone, M.; Vicente-Serrano, S.M.; Alejo-Cochachin, J., (2017). Hydrological and depositional processes associated with recent glacier recession in Yanamarey catchment, Cordillera Blanca (Peru). Sci. Total Environ., 579: 272-282 **(12 pages).**

Malerba, M.E.; Duarte de Paula Costa, M.; Friess, D.A.; Schuster, L.; Young, M.A.; Lagomasino, D.; Serrano, O.; Hickey, S.M.; York, P.H.; Rasheed, M.; Lefcheck, J.S.; Radford, B.; Atwood, T.B.; Ierodiaconou, D.; Macreadie, P., (2023). Remote sensing for cost-effective blue carbon accounting. Earth-Sci. Rev., 238: 104337 **(16 pages).**

Masocha, B.L.; Mhangara, P., (2025). Satellite-driven assessment of methane trends, seasonal variability, and emission hotspots in Botswana's Central and Ngamiland Regions. Environ. Monit. Assess., 197(10): 1-18 **(18 pages).**

Ngoc Tu, N.; Lü, H.; He, W.; Xu, P.; Zhao, M.; Liu, S.; Zhu, Y.; Lei, X., (2025). Automated machine learning integrating multi-source satellite observations to predict gross and net CO2 fluxes of coastal wetlands in China. Environ. Res. Lett., 20: 084011 **(17 pages).**

Ouattara, B., Thiel, M., Forkuor, G., Mouillot, F., Laris, P., Tondoh, E. J., & Sponholz, B. (2025). Fire Impacts, vegetation Recovery, and environmental drivers in West African savannas (2014–2023): A High-Resolution remote sensing assessment. International Journal of Applied Earth Observation and Geoinformation, 143, 1–22 **(22 pages)**.

Padhy, S.R., Bhattacharyya, P., Dash, P.K., Reddy, C.S., Chakraborty, A. and Pathak, H., (2020), Seasonal fluctuation in three mode of greenhouse gases emission in relation to soil labile carbon pools in degraded mangrove, Sundarban, India. Sci. Total Environ., 705:135909 **(12 pages)**.

Peña, E.J.; Sandoval, H.; Zuñiga, O.; Torres, M., (2009). Estimates of carbon reservoirs in high-altitude wetlands in the Colombian Andes. J. Agric. Rural Dev. Trop. Subtrop., 110(2): 115-126 **(12 pages)**.

Senger, D.F.; Saavedra Hortua, D.A.; Engel, S.; Schnurawa, M.; Moosdorf, N.; Gillis, L.G., (2021). Impacts of wetland dieback on carbon dynamics: A comparison between intact and degraded mangroves. Sci. Total Environ., 753: 141817 **(13 pages)**.

Shinkarenko, S.S.; Bartalev, S.A., (2025). Application of remote sensing data in large-scale monitoring of wetlands. Cosmic Res., 62(1): S100-S114 **(15 pages)**.

Suárez Duque, D.; Acurio, C.; Chimbolema, S.; Aguirre, X., (2016). Análisis del carbono secuestrado en humedales altoandinos de dos áreas protegidas del Ecuador. Ecol. Apl., 15(2): 171-177 **(07 pages)**.

Syamdidi; Putri, M.R.; Bernawis, L.I; Wahyudin, R.A.; Trenggono, S.W.; Diantara, S.D.; Yuwono, T.; Sakti, W.I.; Arthatiani, F.Y.; Simamora, D.C.; Sabina, A.; Wahid, L.O.M.A.; Radiarta, I.N., Kasim, K., (2026). Temporal and seasonal influences concerning the carbon footprint of pelagic fisheries. Global J. Environ. Sci. Manage., 12(3): 1169-1190 **(22 pages).**

Vorobyev, S.N.; Kolesnichenko, L.G.; Kolesnichenko, Y.; Prokushkin, A.S.; Lugovaya-Dolmatova, A.V.; Karlsson, J.; Pokrovsky, O.S., (2024). Floodplain carbon dioxide emissions strongly exceed those of the main river stem: A case study of the Ob River, western Siberia. J. Hydrol., 638: 131468 **(12 pages)**.

Vuille, M.; Carey, M.; Huggel, C.; Buytaert, W.; Rabatel, A.; Jacobsen, D.; Soruco, A.; et Villacis, M.; Yarleque, C.; Elison Timm, O.; Condom, T.; Salzmann, N.; Sicart, J.E., (2018). Rapid decline of snow and ice in the tropical Andes: Impacts, uncertainties and challenges ahead. Earth-Sci. Rev., 176: 195-213 **(19 pages)**.

Wang, J.; Yu, G.; Han, L.; Yao, Y.; Sun, M.; Yan, Z., (2024). Ecosystem carbon exchange across China's coastal wetlands: Spatial patterns, mechanisms, and magnitudes. Agric. For. Meteorol., 345: 109859 **(11 pages)**.

Wannasiri, W.; Chaksan, A., (2023). Land use change monitoring systems for spatial GHG emissions and removals assessment in Chiang-Mai, Thailand. Chem. Eng. Trans., 106: 655-660. **(06 pages)**.

Wicaksono, P.; Danoedoro, P.; Hartono; Nehren, U., (2016). Mangrove biomass carbon stock mapping of the Karimunjawa Islands using multispectral remote sensing. Int. J. Remote Sens., 37(1): 26-52 **(27 pages)**.

Withaningsih, S.; Nurmilah, S.; Utama, G.L., (2026). The role of carbon sequestration and biodiversity in agroforestry for climate change mitigation. Global J. Environ. Sci. Manage., 12(1): 431-452 **(22 pages).**

Zhang, Q.; Wei, S.; Chu, X.; Zhang, X.; Gong, Z.; Wang, X.; Song, W.; Xie, B.; Han, G., (2025a). Climate and vegetation jointly determine the interannual variation of net ecosystem CO2 fluxes over 12 years in a restored coastal wetland. Agric. For. Meteorol., 373: 110760 **(10 pages)**.

Zhang, Y.; Lin, W.; Ye, Y.; Li, Y., (2025b). Accounting for land use carbon emissions considering differences in wetland types to support the achievement of SDG 13.2.2. Land Degrad. Dev., 36(4): 1106-1120 **(15 pages)**.

AUTHOR (S) BIOSKETCHES

Mamani-Arpasi, Y., M.Sc., Researcher, Universidad Nacional de Juliaca, San Román 21101, Peru.
- Email: *ymmamania.doc@unaj.edu.pe*
- ORCID: 0000-0002-5643-4516
- Web of Science ResearcherID: QUU-4958-2026
- Scopus Author ID: NA
- Homepage: https://dina.concytec.gob.pe/appDirectorioCTI/VerDatosInvestigador.do?id_investigador=67262

Mamani Gomez, J.A., Ph.D., Professor, Institute for Research in Water Science and Technology, National University of the Altiplano, Puno 21001, Peru; Faculty of Civil Engineering, Architecture and Urbanism, State University of Campinas, Campinas 13083-970, Brazil.
- Email: *jmamani@unap.edu.pe*
- ORCID: 0000-0001-7694-7549
- Web of Science ResearcherID: HSD-9922-2023
- Scopus Author ID: 57193374056
- Homepage: https://ctivitae.concytec.gob.pe/appDirectorioCTI/VerDatosInvestigador.do?id_investigador=0034104

Huanca Chambi, G., M.Sc., Researcher, Universidad Nacional de Juliaca, San Román 21101, Peru.
- Email: *g.huancac@unaj.edu.pe*
- ORCID: 0000-0003-0107-8056
- Web of Science ResearcherID: NA
- Scopus Author ID: NA
- Homepage:https://ctivitae.concytec.gob.pe/appDirectorioCTI/VerDatosInvestigador.do?id_investigador=174664

Quispe Tisnado, M., M.Sc., Researcher, Universidad Nacional de Juliaca, San Román 21101, Peru.
- Email: *miltonqtisnado@gmail.com*
- ORCID: 0009-0001-7744-5935
- Web of Science ResearcherID: NA
- Scopus Author ID: NA
- Homepage: https://ctivitae.concytec.gob.pe/appDirectorioCTI/VerDatosInvestigador.do?id_investigador=222452

Yupanqui Bendita, C.E., M.Sc., Researcher, Universidad Nacional de Juliaca, San Román 21101, Peru.
- Email: *ucesareyb@gmail.com*
- ORCID: 0000-0002-7750-7016
- Web of Science ResearcherID: NA
- Scopus Author ID: 59975381800
- Homepage: https://ctivitae.concytec.gob.pe/appDirectorioCTI/VerDatosInvestigador.do?id_investigador=96030

Calizaya Chura, E., M.Sc., Researcher, Universidad Nacional de Juliaca, San Román 21101, Peru.
- Email: *edgarclzy@gmail.com*
- ORCID: 0009-0007-4060-2670
- Web of Science ResearcherID: NA
- Scopus Author ID: 59976620700
- Homepage:https://ctivitae.concytec.gob.pe/appDirectorioCTI/VerDatosInvestigador.do?id_investigador=472633

Moreno Terrazas, E.G., Ph.D., Professor, Faculty of Biological Sciences, National University of the Altiplano, Puno 21001, Peru.
- Email: *emoreno@unap.edu.pe*
- ORCID: 0000-0001-6356-8806
- Web of Science ResearcherID: HPE-0519-2023
- Scopus Author ID: 57221246484
- Homepage: https://ctivitae.concytec.gob.pe/appDirectorioCTI/VerDatosInvestigador.do?id_investigador=40556

HOW TO CITE THIS ARTICLE:
Mamani-Arpasi, Y.; Mamani Gomez, J.A.; Huanca Chambi, G.; Quispe Tisnado, M.; Yupanqui Bendita, C.E.; Calizaya Chura, E.; Moreno Terrazas, E.G., (2027). Satellite-based assessment of high Andean wetlands and carbon sequestration under the influence of climate change. Global J. Environ. Sci. Manage., 13(1): 123-140.

DOI: 10.22034/gjesm.2027.01.06
URL: https://www.gjesm.net/article_735656.html